

Quantum Phase Transition in One-Dimensional Arrays of Resistively Shunted Small Josephson Junctions

Hisao Miyazaki, Yamaguchi Takahide, Akinobu Kanda, and Youiti Ootuka

Institute of Physics, University of Tsukuba, 1-1-1 Tennodai, Tsukuba, 305-8571, Japan

CREST, Japan Science and Technology Corporation, 4-1-8, Honcho, Kawaguchi, 332-0012, Japan

(Received 22 March 2002; published 18 October 2002)

We have observed a superconductor-insulator transition in one-dimensional (1D) arrays of small Josephson junctions by changing both the resistance R_S of normal metal resistors shunting each junction and the ratio of the Josephson coupling energy E_J to the charging energy E_C . The phase boundary lies at $R_S \approx R_Q$ ($R_Q \equiv h/4e^2 = 6.45 \text{ k}\Omega$) when E_J/E_C is smaller than about unity. We discuss the obtained phase diagram in terms of theoretical models of the dissipation-driven quantum phase transition, with particular attention to differences from 2D arrays.

DOI: 10.1103/PhysRevLett.89.197001

PACS numbers: 74.50.+r, 73.23.Hk, 73.43.Nq

Quantum phase transitions have attracted considerable attention in recent years because they are a key concept in the study of electrical and magnetic properties of various condensed matter systems [1]. The transitions occur at zero temperature and are driven by quantum fluctuations, the magnitude of which varies with a control parameter such as pressure or magnetic field. Josephson junction arrays show a typical example of this kind of transition. The phases of superconducting order parameters of island electrodes in the arrays can be regarded as XY spins, where the Josephson coupling energy E_J represents the coupling between the neighboring spins, and the charging energy E_C determines the strength of the quantum fluctuations. A decrease in a control parameter E_J/E_C leads to a transition from an ordered to a quantum disordered state of the phases, which corresponds to a superconductor-insulator (SI) transition of the array.

In contrast to real spin systems such as magnetic compounds, the arrays can be fabricated with well-controlled parameters of junctions and with the arrangement of junctions designed at will. In addition, what is unique about this system is that an SI transition is also predicted to occur when the strength of coupling of the phases to a dissipative environment is varied. According to the resistively shunted-junction (RSJ) model, the classical dynamics of the phases are damped by dissipative forces inversely proportional to the resistance R_S of Ohmic resistors shunting each junction. The dissipation in a quantum mechanical description [2] damps the quantum fluctuations of the phases, and exceeding a critical value it leads to a superconducting (phase-ordered) state even when E_C is much larger than E_J [3–7]. The dissipation-driven phase transition has been extensively investigated theoretically. Only recently, however, have a quantitative control of dissipation and an observation of the transition been achieved, and that only for 2D arrays [8,9]. It is predicted that the phase diagram at $T = 0$ depends strongly on the dimensionality of the system; a larger

insulating region is expected for lower dimensions because of stronger quantum fluctuations [3–5].

In this Letter, we report the observation of a dissipation-driven phase transition in 1D small-Josephson-junction arrays. To control the strength of the dissipation, we put resistors made of Cr close to and in parallel with each Al/AlO_x/Al junction. The ratio E_J/E_C was also tuned *in situ*. By electrical measurements at low temperatures, the phase diagram of 1D arrays in an E_J/E_C -dissipation plane has been determined experimentally for the first time. The quantitative control of the relevant parameters enabled us to compare the obtained phase diagram directly with theoretically predicted ones and to observe differences from the results of 2D arrays.

The shunted junctions were fabricated using electron-beam lithography and four-angle shadow evaporation with a two-axis rotation stage. For details, see Refs. [9,10]. Neighboring islands are actually connected by two Josephson junctions forming a SQUID loop and by the normal metal resistor (Fig. 1). The SQUID geometry enabled us to tune the effective Josephson coupling E_J between adjacent islands by applying a perpendicular magnetic field B : $E_J = E_J^0 |\cos(\pi BS/\Phi_0)|$. Here, E_J^0 is the Josephson coupling at zero magnetic field, S is the effective area of the SQUID loop, and $\Phi_0 (\equiv h/2e = 2.07 \times 10^{-15} \text{ Wb})$ is the flux quantum. We fabricated an

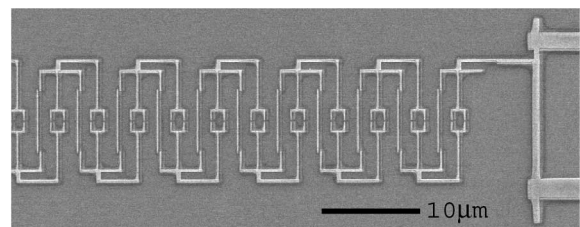


FIG. 1. A scanning electron micrograph of a 1D array with shunt resistors and tunable Josephson couplings.

unshunted array and three arrays with different lengths of Cr strips (2–8 μm) simultaneously on one substrate to obtain a set of arrays with nominally the same junction parameters [11] but with different shunt resistances. We fabricated two such groups (from now on referred to as A and B) of arrays. All the arrays consist of 46 islands. Both voltage probes and current probes for four-terminal measurements were connected to the ends of the arrays. The measurements were performed at temperatures down to 20 mK using a ^3He - ^4He dilution refrigerator.

The parameters of the samples are listed in Table I. The charging energy $E_C(\equiv e^2/2C)$ was determined by the offset voltage in the normal-state IV characteristics. We determine the junction tunnel resistance R_J by dividing the resistance of the unshunted array at 4.2 K by the number of junctions ($=47$). Assuming the arrays on a substrate have the same values of R_J , we estimated the shunt resistance R_S using an equation $R_S = R_J R_{4.2\text{ K}} / (R_J - R_{4.2\text{ K}})$, where $R_{4.2\text{ K}}$ is the resistance per junction of the shunted array at 4.2 K. The value of R_S estimated in this way is consistent with the resistance of the array at the lowest temperature in the magnetic field corresponding to $E_J \approx 0$, which supports the accuracy of the R_S estimation. The Josephson coupling energy E_J^0 was calculated by the Ambegaokar-Baratoff equation $E_J^0 = (R_Q/R_J)(\Delta/2)$, where the Δ is the superconducting energy gap of Al. Using a 3D capacitance extraction program FASTCAP [12], we estimated the self-capacitance C_0 (capacitance of each island to ground) to be 0.37 fF, giving $C/C_0 = 4.6$ for Group A and 6.1 for Group B. The periodic modulation of E_J with applied magnetic field B was confirmed by the oscillation of the zero-bias resistance R_0 for all the arrays. The period ΔB of the oscillation was $(9.34 \pm 0.08) \times 10^{-4}$ T for Group A and $(10.12 \pm 0.11) \times 10^{-4}$ T for Group B, which was consistent with the designed patterns. From now on, we express the perpendicular magnetic field B by the frustration $f \equiv B/\Delta B$.

Figure 2(a) shows temperature dependence of the zero-bias resistance for Group A arrays. The resistance was measured at 10 μV rms (at 21 Hz) for the unshunted array and 9 pA rms for the shunted arrays. The $R_0(T)$ curves clearly show a crossover from insulating to superconducting behavior depending on the value of R_S : The R_0 of the unshunted array increases sharply with decreasing temperature. As the value of R_S is lowered, the increase in R_0 becomes less pronounced, and eventually the R_0 of the array with $R_S = 5.2$ k Ω show a monotonic decrease with decreasing temperature. As shown in Figs. 2(b) and 2(c),

TABLE I. Parameters of the eight arrays. The ∞ means an unshunted array.

	R_S (k Ω)	R_J (k Ω)	E_C/k_B (K)	E_J^0/k_B (K)	E_J^0/E_C
A	$\infty, 17, 11, 5.2$	16	0.55	0.60	1.1
B	$\infty, 15, 6.6, 4.1$	6.2	0.41	1.7	4.2

the current-voltage characteristics also change from showing a Coulomb gap to showing the Josephson-current-like behavior as the value of R_S is decreased.

Figure 3 shows how the $dV/dI - V$ curves of two arrays in Group B change depending on f . The excitation voltage was smaller than 2 μV rms. As shown in Fig. 3(a), the curves for $R_S = 15$ k Ω show a Josephson-current-like behavior, namely, a lower resistance at smaller bias, when $f < 0.30$. On the other hand, a peak (a higher resistance at smaller bias) appears inside the Josephson-current-like region when f exceeds about 0.30. This means Coulomb blockade of Cooper pair tunneling sets in. Since changing f from 0 to 1/2 corresponds to the reduction of E_J from E_J^0 to 0, this is the SI transition depending on the ratio E_J/E_C . The unshunted array and the array with $R_S = 6.6$ k Ω in Group B also show the transition. On the contrary, the array with $R_S = 4.1$ k Ω did not show the insulating behavior even when $f \rightarrow 0.5$, as shown in Fig. 3(b). Thus, whether the SI transition due to the ratio E_J/E_C occurs depends on the values of R_S .

Using the above results, we construct a phase diagram in an $E_J/E_C - R_Q/R_S$ plane in the $T = 0$ limit, which is shown in Fig. 4. Whether the array is insulating or superconducting at $T \rightarrow 0$ is determined by whether the

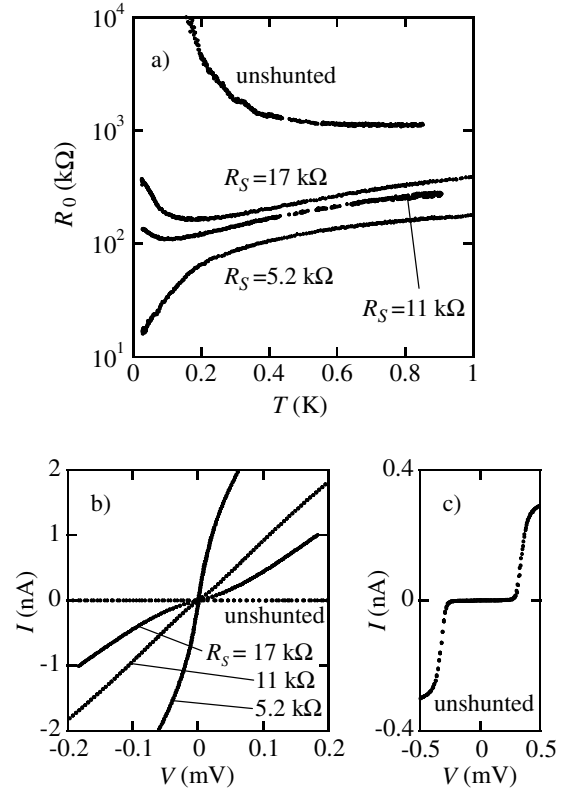


FIG. 2. (a) Temperature dependence of the zero-bias resistance for Group A arrays at $f = 0.00$. The arrays have nominally the same junction tunnel resistance $R_J = 16$ k Ω and the same ratio $E_J/E_C = 1.1$. (b), (c) Current-voltage characteristics for Group A arrays, measured at 25 mK and at $f = 0.00$.

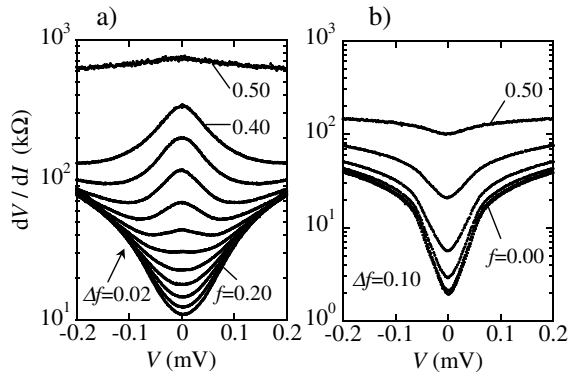


FIG. 3. Differential resistance dV/dI vs voltage V for two arrays in Group B, measured at 20 mK and at several magnetic fields; (a) $R_S = 15$ k Ω , (b) $R_S = 4.1$ k Ω .

$dV/dI - V$ curve at the lowest temperature has a Coulomb-blockade peak or it has only a Josephson-current-like structure. Each bar in the figure represents the states of an array at various values of E_J which is tuned by the applied magnetic field. The phase diagram shows the phase boundary is located at $R_Q/R_S = 0.98$ – 1.2 for small E_J/E_C . In a previous study [9], we determined a phase diagram of resistively shunted 2D arrays, in which the phase boundary was at $R_Q/R_S \approx 0.5$ for small E_J/E_C . Both the results for 1D and 2D arrays are explained consistently by the theories of the dissipation-driven phase transition, which predict that the critical value of R_Q/R_S for d -dimensional cubic arrays is $1/d$ when $E_J/E_C \rightarrow 0$ [3–5]. Another notable feature is that the phase boundary of the 1D arrays near the $R_Q/R_S = 0$ axis appears to be at one order of magnitude larger value of E_J/E_C than that (≈ 0.6) of the 2D arrays

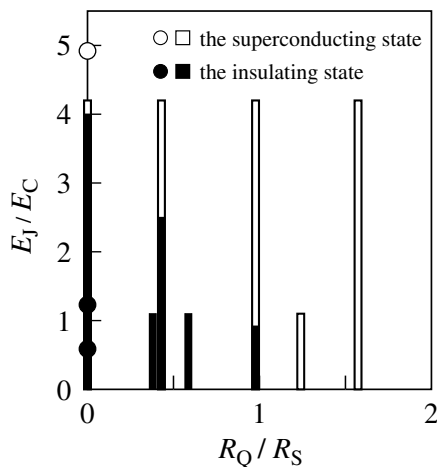


FIG. 4. Phase diagram in the $E_J/E_C - R_Q/R_S$ plane in the $T = 0$ limit. A change from white to black in the middle of a bar corresponds to the SI transition depending on f , e.g., shown in Fig. 3(a). The circles show the results of another experiment in which we used unshunted junction arrays having no SQUID geometry and, hence, having constant values of E_J .

[9,13]. This is consistent with the intuitive expectation that the system with lower dimension has a stronger quantum fluctuation and, hence, a stronger tendency to become insulating.

Quantitatively, however, theoretical models have predicted a still larger difference in the position of the phase boundary between 1D and 2D arrays. According to theories [3,6], 1D arrays should be insulating at $R_Q/R_S < 1$ and superconducting at $R_Q/R_S > 1$ regardless of the ratio E_J/E_C if the charging energy is associated only with the junction capacitances. This is in marked contrast to 2D arrays, the insulating state of which is predicted to appear only in the lower-left corner of the phase diagram, namely, at R_Q/R_S smaller than 0.5 and E_J/E_C smaller than order 10^{-1} [3,14]. Theoretical models taking into account the self-capacitances predict that the insulating region of 1D arrays is also limited to the small E_J/E_C region, with a critical point $(E_J/E_C)_{cr} \geq 3.2C/C_0$ at $R_Q/R_S = 0$ [7]. Figure 4 shows, however, that the phase boundary on the $R_Q/R_S = 0$ axis appears to be at $E_J/E_C = 4$, which is smaller than the predicted limiting value $3.2C/C_0 = 20$ for Group B. Experiments on 1D *unshunted* arrays performed by other groups also show the discrepancy in the position of the phase boundary between theory and experiment: The phase boundaries were reported to be at $E_J/E_C = 3.0$ [15], 2.2 [16], and 3.5–4.2 [17]. These values are also smaller than the predicted limiting values, which is 1.1 – 1.4×10^3 [18] for the arrays of Ref. [16]. The shrinkage in the insulating region may result from the limitation in voltage measurements and/or the thermal fluctuation that would hinder the observation of the Coulomb-blockade gap, as has been suggested for single shunted junctions [19]. Incidentally, combining our results with those of Refs. [15–17], we find that the position of the phase boundary at $R_Q/R_S = 0$ does not depend very much on the value of C/C_0 .

It is predicted from the nature of the XY model that the superconducting state (a vanishing zero-bias resistance) of 1D arrays emerges only at *zero* temperature [3,5,7]. This is again in contrast to 2D arrays, the superconducting state of which could emerge at *finite* temperatures below a critical temperature [14]. From this viewpoint, it is interesting to explore how the 1D “superconducting” (meaning $R_0 = 0$ at $T = 0$) arrays go into the $R_0 = 0$ state as the temperature is decreased.

The dots in Fig. 5(a) show the temperature dependence of zero-bias resistance R_0 (actually, measured at 10 pA rms) for the array with $R_S = 5.2$ k Ω in Group A at four different f . The data show approximate power-law behavior. The filled symbols in Fig. 5(b) show the power-law exponent plotted as a function of E_J/E_C [20]. An interesting finding is that when the IV curve at the lowest temperature is plotted in the form of $V/I(\Omega)$ vs $\hbar/e k_B$ (K), the data fall on the $R_0(T)$ curve, as shown in Fig. 5(a). These are partly explained by a theory considering quantum phase slip for each junction, i.e., quantum tunneling with dissipation in the tilted washboard potential [7,21]. It

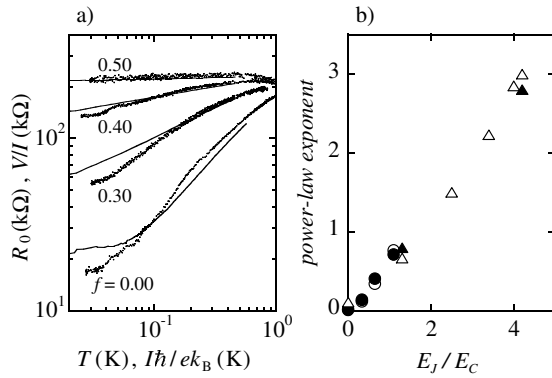


FIG. 5. (a) Zero-bias resistance as a function of temperature (dots) and V/I as a function of current at 26 mK (continuous lines) for the array with $R_S = 5.2$ kΩ in Group A. The current is converted to temperature by the factor \hbar/ek_B . (b) The power-law exponents of the R_0-T curves (filled symbols) and the $V/I-I$ curves (open symbols), plotted as a function of E_J/E_C . Circles and triangles represent the data points for the array with $R_S = 5.2$ kΩ in Group A and the array with $R_S = 4.1$ kΩ in Group B, respectively.

predicts that V/I (i.e., the phase mobility) depends algebraically on both temperature T and the current I (i.e., the slope of the potential), namely, $V/I \propto T^\lambda (k_B T \gg \hbar/e)$ and $V/I \propto I^\lambda (k_B T \ll \hbar/e)$, where the exponents are the same for both cases. This explains the same power-law behavior for the R_0-T and $V/I-I$ curves. Figure 5(b) shows that the exponent becomes zero when $E_J/E_C \rightarrow 0$, corresponding to the fact that V/I hardly depends on T and I at $f = 0.50$ as shown in Fig. 5(a). This is naturally understood because at $f = 1/2$ the Josephson coupling disappears and the electric properties of only shunt resistors can be observed, i.e., $V/I \approx 47R_S$. In Fig. 5(b) one can also see that the exponent for $R_S = 5.2$ kΩ does not differ very much from that for $R_S = 4.1$ kΩ. This observation cannot be explained by the theory, which predicts that $\lambda = 2(R_0/R_S - 1)$ when $E_J/E_C \rightarrow 0$, but this may be because the expression is derived in the low temperature limit: $k_B T \ll E_C(E_J/E_C)^{R_0/(R_0-R_S)}$ [22]. Further work, in particular, in a larger R_0/R_S regime, will lead to a more detailed understanding of the finite temperature dynamics.

We thank S. E. Korshunov and T. Kato for useful discussions. This work was supported in part by a Grant-in-Aid for Scientific Research from the Japan Ministry of Education, Science, Sports, and Culture. Y.T. acknowledges the support from the Japan Society for the Promotion of Science.

[1] S. Sachdev, *Quantum Phase Transitions* (Cambridge University Press, Cambridge, 2000).

[2] A. O. Caldeira and A. J. Leggett, *Ann. Phys. (N.Y.)* **149**, 374 (1983).

[3] M. P. A. Fisher, *Phys. Rev. B* **36**, 1917 (1987).
 [4] S. Chakravarty, G.-L. Ingold, S. Kivelson, and G. Zimanyi, *Phys. Rev. B* **37**, 3283 (1988).
 [5] A. Kampf and G. Schön, *Phys. Rev. B* **36**, 3651 (1987).
 [6] P. A. Bobbert, R. Fazio, G. Schön, and A. D. Zaikin, *Phys. Rev. B* **45**, 2294 (1992).
 [7] S. E. Korshunov, *Europhys. Lett.* **9**, 107 (1989); **9**, 839(E) (1989); *Sov. Phys. JETP* **68**, 609 (1989).
 [8] A. J. Rimberg, T. R. Ho, C. Kurdak, J. Clarke, K. L. Campman, and A. C. Gossard, *Phys. Rev. Lett.* **78**, 2632 (1997).
 [9] Y. Takahide, R. Yagi, A. Kanda, Y. Ootuka, and S. Kobayashi, *Phys. Rev. Lett.* **85**, 1974 (2000); T. Yamaguchi *et al.*, *Physica (Amsterdam)* **352C**, 181 (2001).
 [10] R. Yagi and S. Kobayashi, *J. Phys. Soc. Jpn.* **66**, 3360 (1997); R. Yagi *et al.*, *ibid.* **66**, 3722 (1997).
 [11] Our previous experiments show a maximum variation of $\pm 5\%$ in the normalized resistance per junction, measured at 4.2 K, for arrays fabricated on one substrate: T. Yamaguchi *et al.*, *J. Phys. Soc. Jpn.* **67**, 729 (1998); **65**, 2365 (1996).
 [12] K. Nabors and J. White, *IEEE Trans. Comput.-Aided Des.* **10**, 1447 (1991). We assumed a conductor with the same geometry as the actual array, surrounded by a dielectric medium with an effective dielectric constant of 6.45, an average between the dielectric constant of free space ($=1$) and that of Si ($=11.9$).
 [13] H. S. J. van der Zant, W. J. Elion, L. J. Geerligs, and J. E. Mooij, *Phys. Rev. B* **54**, 10 081 (1996).
 [14] C. Rojas and J. V. José, *Phys. Rev. B* **54**, 12 361 (1996).
 [15] E. Chow, P. Delsing, and D. B. Haviland, *Phys. Rev. Lett.* **81**, 204 (1998).
 [16] D. B. Haviland, K. Andersson, P. Ågren, J. Johansson, V. Schöllmann, and M. Watanabe, *Physica (Amsterdam)* **352C**, 55 (2001).
 [17] W. Kuo and C. D. Chen, *Phys. Rev. Lett.* **87**, 186804 (2001).
 [18] The estimated value of $C_0 = 8-10$ aF in Ref. [16] is smaller than ours because of smaller sizes of their islands.
 [19] J. S. Penttilä, Ü. Parts, P. J. Hakonen, M. A. Paalanen, and E. B. Sonin, *Phys. Rev. Lett.* **82**, 1004 (1999); C. P. Herrero and A. D. Zaikin, *Phys. Rev. B* **65**, 104516 (2002).
 [20] The R_0 of the array with $R_S = 4.1$ kΩ in Group B falls algebraically with exponent shown in Fig. 5(b) but becomes temperature independent at $T < 0.2$ K, as has been observed in the previous measurements on unshunted arrays. The flattening of the $R_0(T)$ curve may be attributed to the finite length of the array [15], the effect of which is stronger for arrays with larger values of $\sqrt{8E_J E_{C0}}$ ($E_{C0} \equiv e^2/2C_0$).
 [21] S. E. Korshunov, *Sov. Phys. JETP* **65**, 1025 (1987); G. Schön and A. D. Zaikin, *Phys. Rep.* **198**, 237 (1990).
 [22] S. E. Korshunov (private communication).